9-3-2004

Amyloid directly inhibits human alpha4beta2-nicotinic acetylcholine receptors heterologously expressed in human SH-EP1 cells

J. Wu

Y-P Kuo

L. Xu

J. B. Eaton

L. Zhao

See next page for additional authors

Authors
J. Wu, Y-P Kuo, L. Xu, J. B. Eaton, L. Zhao, J. Wu, and R. J. Lukas

THE JOURNAL OF BIOLOGICAL CHEMISTRY
Vol. 279, No. 36, Issue of September 3, pp. 37842–37851, 2004
Printed in U.S.A.

β-Amyloid Directly Inhibits Human α4β2-Nicotinic Acetylcholine Receptors Heterologously Expressed in Human SH-EP1 Cells*

Received for publication, January 13, 2004, and in revised form, July 1, 2004
Published, JBC Papers in Press, July 2, 2004, DOI 10.1074/jbc.M400335200

Jie Wu‡§, Yen-Ping Kuo¶, Andrew A. George¶, Lin Xu¶, Jun Hu‡, and Ronald J. Lukas¶

From the ‡Division of Neurology and the ¶Division of Neurobiology, Barrow Neurological Institute, St. Joseph's Hospital and Medical Center, Phoenix, Arizona 85013-4496

Amyloid-β (Aβ) accumulation and aggregation are thought to contribute to the pathogenesis of Alzheimer's disease (AD). In AD, there is a selective decrease in the numbers of radioligand binding sites corresponding to the most abundant nicotinic acetylcholine receptor (nAChR) subtype, which contains human α4 and β2 subunits (hα4β2-nAChR). However, the relationships between these phenomena are uncertain, and effects of Aβ on hα4β2-nAChR function have not been investigated in detail. We first confirmed expression of hα4 and hβ2 subunits as messenger RNA in transfected, human SH-EP1 cells by reverse transcription-polymerase chain reaction and mRNA fluorescence *in situ* hybridization analyses. Immunoprecipitation Western analyses confirmed α4 and β2 subunit protein expression and co-assembly. Whole cell current recording demonstrated heterologous expression in SH-EP1-hα4β2 cells of functional hα4β2-nAChRs with characteristic responses to nicotinic agonists or antagonists. Nicotine-induced whole cell currents were suppressed by $A\beta_{1-42}$ in a dose-dependent manner. Functional inhibition was selective for $A\beta_{1-42}$ compared with the functionally inactive, control peptide $A\beta_{40-1}$. $A\beta_{1-42}$-mediated inhibition of hα4β2-nAChR function was non-competitive, voltage-independent, and use-independent. Pre-loading of cells with guanyl-5′-yl thiophosphate failed to prevent $A\beta_{1-42}$-induced inhibition, suggesting that down-regulation of hα4β2-nAChR function by $A\beta_{1-42}$ is not mediated by nAChR internalization. Sensitivity to $A\beta_{1-42}$ antagonism at 1 nM was evident for hα4β2-nAChRs, but not for heterologously expressed human α7-nAChRs, although both nAChR subtypes were functionally inhibited by 100 nM $A\beta_{1-42}$, with the magnitude of functional block being higher for 100 nM $A\beta_{1-42}$ acting on hα7-nAChRs. These findings suggest that hα4β2-nAChRs are sensitive and perhaps pathophysiologically relevant targets for Aβ neurotoxicity in AD.

* This work was supported by an Arizona Alzheimer's Disease Center pilot grant and the Marjorie Newsome and Sandra Solheim Aiken fund (to J. W.). Other work toward this project, part of which was conducted in the Charlotte and Harold Simensky Neurochemistry of Alzheimer's Disease Laboratory, was supported by endowment and/or capitalization funds from the Men's and Women's Boards of the Barrow Neurological Foundation, the Robert and Gloria Wallace Foundation, Arizona Disease Control Research Commission Grants 9615 and 1-353, and National Institutes of Health Grant NS040417 (to R. J. L.). The costs of publication of this article were defrayed in part by the payment of page charges. This article must therefore be hereby marked "*advertisement*" in accordance with 18 U.S.C. Section 1734 solely to indicate this fact.

§ To whom correspondence should be addressed: Division of Neurology, Barrow Neurological Institute, St. Joseph's Hospital and Medical Center, 350 West Thomas Rd., Phoenix, AZ 85013-4496. Tel.: 602-406-6376; Fax: 602-406-7172; E-mail: jwu2@chw.edu.

Alzheimer's disease (AD)[1] is a progressive, neurodegenerative disorder manifest as a severe impairment of learning and memory. Pathophysiological hallmarks of AD include extracellular deposits of β-amyloid peptide (Aβ) in senile plaques, formation of intraneuronal neurofibrillary tangles, and cholinergic neuron death (1). Although the precise mechanisms of AD pathogenesis are only partially understood, it is now widely accepted that the accumulation and aggregation of $A\beta_{1-42}$ plays a key role in the disease (2). Evidence has indicated an interaction between Aβ and the cholinergic system (3). For example, very low concentrations (pico to nanomolar) of Aβ can directly induce cholinergic hypofunction (4–6). It has been reported that solubilized Aβ inhibits several steps of acetylcholine synthesis and release (4, 7), inhibits cholinergic enzyme activity (6), impairs cholinergic metabolism and neurotransmission (8–10), and depresses hippocampal synaptic function (11).

Recent evidence suggests possible roles for nicotinic acetylcholine receptors (nAChRs) as central targets for Aβ-induced neurotoxicity manifest as cholinergic hypofunction and cognitive impairment. First, in the brain of AD patients, there is a marked decrease in the numbers of nAChR radioligand binding sites (12), particularly those that have the highest affinity for nicotine and appear to be the most abundant nAChR subtype in the brain of vertebrates (13–16). Immunoassays show that these nAChRs contain α4 and β2 subunits (17, 18). Second, nAChR α4 and β2 subunit immunoreactivity is localized in AD brain to Aβ plaques and neurofibrillary tangles (19). Third, interactions have been reported of $A\beta_{1-42}$ with radioligand binding sites on another abundant nAChR subtype found in the vertebrate brain containing α7 subunits (α7-nAChR; picomolar affinity) and on presumed α4β2-nAChR subtypes (nanomolar affinity) (20, 21). Direct inhibition to some extent of α7-nAChR function by Aβ has been demonstrated in whole cell current and excised membrane patch single channel recordings from interneurons in rat hippocampal slices (22), in whole cell studies using rat hippocampal cultured neurons (23), and in whole cell recordings from *Xenopus* oocytes containing heterologously expressed rat or human α7-nAChRs (24, 25), although one report describes that picomolar concentrations of Aβ directly activated whole cell current responses of *Xenopus* oocytes heterologously expressing rat α7-nAChRs (26). Fourth, it is well known that nAChRs participate in cognitive functions, including learning and memory (16), which are compromised in animals lacking α4 or β2 subunits (27, 28). Thus, nAChR agonists,

[1] The abbreviations used are: AD, Alzheimer's disease; Aβ, β-amyloid peptides; ACh, acetylcholine; DHβE, dihydro-β-erythroidine; hα4β2-nAChR, human nAChR composed of α4 and β2 subunits; nAChR(s), nicotinic acetylcholine receptor(s); PBS, phosphate-buffered saline; RT, reverse transcription; GAPDH, glyceraldehyde-3-phosphate dehydrogenase; GDPβS, guanyl-5′-yl thiophosphate; β2ch, chimeric β2.

antagonists, and modulators have received attention as potentially novel agents for therapeutic use in AD (29–31).

However, surprisingly little attention has been given to the possible functional effects of Aβ on the function of human (h) α4β2-nAChRs. To fill this gap in knowledge, we employed patch clamp techniques to elucidate the acute effects of $A\beta_{1-42}$, control peptide, or related peptides on the function of hα4β2-nAChRs heterologously expressed in the SH-EP1 cell line.

EXPERIMENTAL PROCEDURES

Heterologously Expressed hα4β2-nAChRs in SH-EP1 Cells—Human α4 and β2 subunits (kindly provided by Dr. Ortrud Steinlein, Institute for Human Genetics, Rheinische-Wilhelms-Universitat, Bonn, Germany) were subcloned into pcDNA3.1-zeocin and pcDNA3.1-hygromycin vectors, respectively, and transfected using established techniques (32–34) into native nAChR-null SH-EP1 cells (35) to create the SH-EP1-hα4β2 cell line. For this and all other methods, manipulations were conducted at room temperature (23 ± 1 °C) unless otherwise noted. Briefly, 3 million SH-EP1 cells in 0.5 ml of 20 mM HEPES, 87 mM NaCl, 5 mM KCl, 0.7 mM $NaHPO_4$, 6 mM dextrose, pH 7.05, in an electroporation cuvette were mixed with 100 μg of α4 and β2 subunit cDNA constructs. Samples were subjected to electroporation (Bio-Rad Gene Pulsar model 1652076) at 960 microfarads and 200 volts. After electroporation, cells were suspended to 5 ml in complete medium (36), and 1-ml aliquots were added to 12-ml aliquots of medium in each of five 100-mm dishes before returning the cells to an incubator at 37 °C. 48 h later, positive selection of incubated cells was initiated by supplementing the medium with 0.25 mg/ml zeocin (Invitrogen) and 0.4 mg/ml hygromycin (Calbiochem). Colonies of surviving cells were picked by ring cloning and expanded before being screened for radioligand binding and functional evidence for α4β2-nAChR expression, which led to selection of the clone designated as the SH-EP1-hα4β2 cell line. Cells were maintained as low passage in medium with 0.25 mg/ml zeocin and 0.4 mg/ml hygromycin to ensure stable expression of phenotype and passaged once weekly by splitting just-confluent cultures 1/10 to maintain cells in proliferative growth. Studies also were done using another cell line transfected with the human α4 subunit cDNA and a chimeric β2 subunit cDNA encoding nAChR β2 subunit sequences, except for cytoplasmic loop amino acids sequence Lys^{336}-Ser^{448}, which was replaced by amino acids Arg^{347}-Ala^{448} from the murine serotonin receptor 5-TH_{3A} subunit sequence via a process described in detail elsewhere (37).

RNA Preparation and Reverse Transcription (RT)-PCR—Total RNA was isolated from the cells growing at ~80% confluency in a 100-mm culture dish using 2 ml of TRIzol™ reagent (Invitrogen). Prior to RT-PCR, RNA preparations were treated with amplification-grade RNase-free DNase (Invitrogen) to remove residual genomic DNA contamination. Typically, 1 μg of RNA was incubated with 1 unit of DNase I in a 10 μl-reaction at room temperature for 15 min, and the DNase I was subsequently inactivated by addition of 1 μl of 25 mM EDTA and incubation at 65 °C for 10 min. RT was carried out using 0.8 μg of DNA-free total RNA and oligo$(dT)_{12-18}$ primer in a 20-μl reaction using the Superscript II™ Preamplification system (Invitrogen). At the end of the RT reaction, reverse transcriptase was deactivated by incubation at 75 °C for 10 min, and RNAs were removed by adding 1 unit of RNase H followed by incubation at 37 °C for 30 min. A typical PCR was performed using 2 μl of cDNA preparation, 1 μl of 10 μM each of 5′ and 3′ gene-specific primers, 1 μl of 10 mM dNTP, and 2.5 units of RedTaq™ (Sigma) in a 50-μl reaction. The primers used in the amplification stage were designed and synthesized based on published gene sequences (GenBank™ accession numbers: α4, L35901; β2, X53179; GAPDH, M32599). The primer sequences and their predicted product sizes are: nAChR, α4 subunit sense 5′-gaatgtcacctccatccgcatc-3′, α4 antisense 5′-ccggca(a/g)ttgtc(c/t)ttgaccac-3′ (product size 790 bp); nAChR, β2 subunit sense 5′-cggctcccttccaaacaca-3′, β2 antisense 5′-gcaatgatggcgtggctgctgca-3′ (product size 754 bp); GAPDH, sense 5′-cgtattgggcgcctggtcaccag-3′, GAPDH antisense 5′-gtccttgcccacagccttggcagc-3′ (product size 624 bp). Amplification reactions were carried out in a RoboCycler (Stratagene, La Jolla, CA) for 35 amplification cycles at 95 °C for 1 min, 55 °C for 90 s, and 72 °C for 90 s, followed by an additional 4-min extension at 72 °C. One-tenth of each RT-PCR product was then resolved on a 1% agarose gel before ethidium staining was used to visualize bands under ultraviolet illumination.

In Situ Hybridization for Cell-specific Localization of α4 or β2 Subunit Message—Riboprobes corresponding to nucleotide sequences coding for large segments of the α4 or β2 subunit large cytoplasmic domains were prepared from *in vitro* transcription and used for *in situ* hybridization. For riboprobe preparation, 354- (for the α4 subunit) or 211-bp (for the β2 subunit) partial cDNA fragments were amplified from human nAChR α4 and β2 subunit cDNA constructs using the following two sets of PCR primers: α4 sense 5′-gcacccgccctcaccgtccttc-3′ and α4 antisense 5′-tcagccgagtgggtgttgcgagag-3′; β2 sense 5′-catcattgcgcccgtcagcg-3′ and β2 antisense 5′-gccacagccacacggctccc-3′. These α4 and β2 subunit cytoplasmic domain templates were then gel purified and non-directionally ligated to a T7 phage promoter adapter (Lig'n Scribe, Ambion, Austin, TX). Subsequent PCRs using sense or antisense gene-specific primers in conjunction with Lig'n Scribe adapter primers were then performed to selectively amplify ligation products of *in vitro* transcription templates in antisense or sense orientation. Sense or antisense partial α4/β2 RNAs were separately transcribed from the PCR-derived template in the presence of biotinylated UTPs using the MAXIscript *in vitro* transcription system (Ambion), and the quality and quantity of the riboprobes were evaluated using denaturing polyacrylamide gel electrophoresis and spectrophotometric reading, respectively. For cell sample preparation, confluent SH-EP1-hα4β2 cells were trypsinized, resuspended in medium, seeded on Lab Tek II CC2 chambered slides at a target density of ~50,000 cells/chamber, and allowed to grow at 37 °C to achieve proper morphology and optimal confluence (~90%). After ~2 days, cells were then briefly rinsed in 1× phosphate-buffered saline (PBS), fixed in 4% paraformaldehyde, rinsed again in 1× PBS for 5 min, and acetylated, delipidated with chloroform, and serially dehydrated with ethanol (50, 75, 85, and 95%) at 23 ± 1 °C. Samples were then incubated in pre-hybridization solution containing final concentrations of 250 μg/ml tRNA, 25% formamide, 10% dextran sulfate, 2.5× Denhardt's solution, 0.05 mg/ml salmon sperm DNA, 4× SSCP, 4 mM EDTA, pH 8.0, for 2 h at 50 °C before being incubated in hybridization solution containing antisense or sense probes (final concentration ranging from 0.2 to 0.7 ng/μl) for 20 h at 50 °C. After hybridization, samples were rinsed in 2× SSC twice for 5 min each, 1× SSC for 10 min, 0.5× SSC for 10 min at 23 ± 1 °C, 0.1× SSC for 20 min at 60 °C, and briefly rinsed in double distilled water at 23 ± 1 °C. Samples were then dehydrated again in a graded ethanol series and vacuum dried under desiccant. Dry samples were then rehydrated by rinsing in 1× PBS for 5 min before submersion in a 1:2000 dilution (in 1× PBS supplemented with 0.1% bovine serum albumin) of avidin-Alexa fluorophore complexes (Molecular Probes, Eugene, OR) for 30 min. To terminate the reaction, samples were rinsed 3 times in 1× PBS for 15 min each, again at 23 ± 1 °C. Slides were then coverslipped and stored at 4 °C in the dark until being subjected to fluorescence microscopy (Olympus IX70, Melville, NY) and image analysis using ImagePro Plus version 4.1 (Silver Spring, MD).

Immunoprecipitation-Western Analysis for Confirmation of α4 and β2 Subunit Assembly—Preparation of non-ionic detergent-solubilized membranes for immunoprecipitation began with medium removal from 100-mm dishes containing plated cells, rinsing of dishes 3 times with NP buffer (100 mM NaCl, 25 mM $NaPO_4$, pH 7.4), mechanical harvesting of cells using a rubber policeman, and centrifugation of healthy, confluent cells from the suspension for 5 min at 1,000 × *g*. The cell pellets were then resuspended and homogenized in ice-cold NP buffer (200 μl/confluent plate) supplemented with complete protease inhibitor mixture (1 Mini tablet per 10 ml; Roche Diagnostics), followed by centrifugation at 10,000 × *g* for 10 min at 4 °C. After centrifugation, the supernatant was then discarded and the pellet resuspended in TNP buffer (NP buffer supplemented with 1% Triton X-100; 200 μl per ml of starting suspension; supplemented with protease inhibitor mixture) by incubating at room temperature for 30 min. The preparation was then centrifuged at 12,500 × *g* for 10 min at 4 °C. The supernatant fraction containing the solubilized membrane protein was then collected, and separate samples were reacted overnight at 4 °C with either H133 (rabbit anti-nAChR α4 subunit) or H92 (rabbit anti-nAChR β2 subunit) antibodies (both from Santa Cruz Biotechnology, Santa Cruz, CA; 5 μg/1 mg of solubilized total membrane protein) in the presence of protein G-agarose beads (50 μl; Calbiochem). Immunoprecipitants were collected by centrifugation, and the beads containing immune complexes were washed 3 times in TNP buffer before being resuspended in SDS-PAGE sample buffer containing β-mercaptoethanol (20 μl per sample; ICN Biomedicals), heated to 95 °C for 3 min, and centrifuged briefly to remove the stripped agarose beads. The now-resolubilized protein samples were then collected and subjected to SDS-PAGE separation on 10% acrylamide gels and transferred to nitrocellulose membrane for Western analysis. Membranes were then blocked by PBS buffer containing 5% skim milk powder and incubated with primary monoclonal antibody 299 (rat anti-nAChR α4; 1:1000; Sigma) and pAb s-1724 (rabbit anti-nAChR β2; 1:50; a gift from Dr. J. Patrick, Baylor College of Medicine, Houston, TX) for 1 h. After three 5-min washes in PBS containing 0.05% Tween 20, secondary horseradish peroxidase-

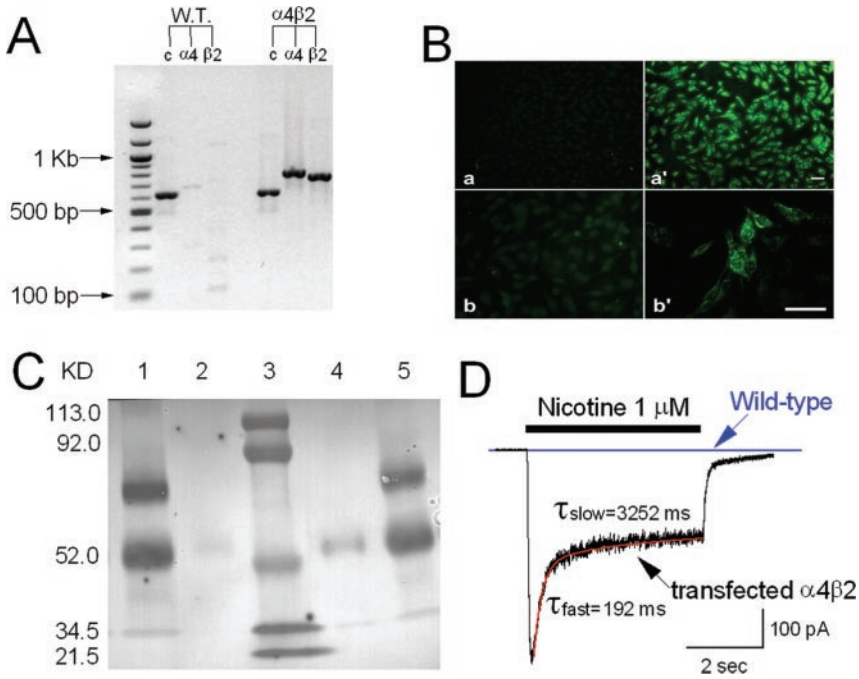

FIG. 1. **Heterologously expressed human α4β2-nAChRs in the SH-EPI cell lines.** *A*, RT-PCR analysis of GAPDH (*lane c*) or nAChR α4 or β2 subunit messenger RNAs from transfected SH-EPI-hα4β2 cells (α4β2) or from untransfected SH-EP1 host cells (*W.T.*) were performed as described under "Experimental Procedures." The RT-PCR products were electrophoretically resolved on a 1% agarose gel along with a 100-bp ladder molecular weight marker. GAPDH serves as a positive control, indicating success of RT-PCR analysis, and specificity of α4 and β2 subunit expression only in transfected cells also is demonstrated. *B*, *in situ* hybridization showing expression of nAChR α4 and β2 subunit transcripts in the SH-EP1-hα4β2 cell line. Following the protocol described under "Experimental Procedures," cells were probed either with biotinylated α4 or β2 sense orientation riboprobes (*a* and *b*, respectively) or with biotinylated antisense α4 or β2 riboprobe (*a′* and *b′*, respectively). The hybridized probes were then labeled with avidin-Alexa 488, and the signal was subjected to epifluorescence microscopic analysis. Images were obtained at ×200 (*a* and *a′*) or ×600 (*b* and *b′*) magnification (*calibration bars* are 20 and 50 μm, respectively). *C*, immunoprecipitation-Western analysis showing nAChR α4 and β2 subunit expression and co-assembly in SH-EP1-hα4β2 cells. Membrane fractions from untransfected SH-EP1 cells (*lanes 2* and *4*) or SH-EP1-hα4β2 cells (*lanes 1* and *5*) were detergent solubilized and subjected to immunoprecipitation using anti-α4 antibody (*lanes 1* and *2*) or anti-β2 antibody (*lanes 4* and *5*) before being subjected to SDS-PAGE, vacuum blotting, and Western analyses for both nAChR α4 subunit (~70 kDa band; compare with pre-stained SDS-PAGE mass standards in *lane 3* having sizes indicated to the *left* of the image) and β2 subunit (~52-kDa band) proteins. The faint band of ~55 kDa in *lanes 2* and *4* is not reproducibly observed and likely reflects cross-reaction of donkey anti-rabbit IgG with primary rabbit anti-subunit antibodies sometimes carried over into the sample. *D*, wild-type, untransfected SH-EP1 cells (*blue arrow*) or SH-EP1-hα4β2 cells heterologously expressing human α4 and β2 subunits (*black arrow*) were tested for whole cell current responses to 1 μM nicotine applied for 4 s. No response was observed in wild-type cells, but an inward current was rapidly induced in transfected cells.

conjugated, goat anti-rat IgG (sc-2006) and donkey anti-rabbit IgG (sc-2313) antibodies (1:1000; Santa Cruz Biotechnology) were added to the reaction medium to allow conjugation with subunit-primary antibody targets. The horseradish peroxidase:second antibody-labeled bands were then visualized by using enhanced substrate Opti-4CN (Bio-Rad). Earlier control studies had demonstrated that there was no cross-reactivity on the nitrocellulose membranes between monoclonal antibody 299 and β2 subunits, between pAb s-1724 and α4 subunits, between secondary antibodies and nAChR subunits, or between goat anti-rat IgG antibody and any residual rabbit antibodies in immunoprecipitates (although cross-reactivity between donkey anti-rabbit IgG and rabbit antibodies carried over from immunoprecipitations was sometimes observed), ensuring that nAChR α4 and β2 subunits could be identified on the same Western blot when probed with both subunit-specific antibodies and both species-specific anti-IgG.

Patch Clamp Whole Cell Current Recordings—Conventional whole cell current recording, coupled with techniques for fast application and removal of drugs (U-tube), was applied in this study as previously described (38–40). Briefly, cells plated on poly-lysine-coated 35-mm culture dishes were placed on the stage of an inverted microscope (Olympus iX7, Lake Success, NY) and continuously superfused with standard external solution (2 ml/min). Glass microelectrodes (3–5 MΩ resistance between pipette and extracellular solutions) were used to form tight seals (>2 GΩ) on the cell surface until suction was applied to convert to conventional whole cell recording. Cells were then voltage-clamped at a holding potential of −60 mV, and ion currents in response to application of ligands were measured (Axon Instruments 200B amplifier, Foster City, CA), typically using data filtered at 2 kHz, acquired at 5 kHz, displayed and digitized on-line (Axon Instruments Digidata 1200 series A/D board), and stored on hard media for subsequent off-line analysis. Both pipette and whole cell current capacitance were minimized, and the series resistance was routinely compensated to 80%. Before series resistance compensation, whole cell access resistance less than 20 MΩ was accepted. Data acquisition and analyses were done using Pclamp8.0 (Axon Instruments), and results were plotted using Origin 5.0 (Microcal, North Hampton, MA). nAChR acute desensitization (the decline in inward current amplitude over the course of agonist application) was analyzed for decay half-time (τ; $\tau = 0.693/k$ for decay rate constant k), peak current (I_p), and steady-state current (I_s), using fits to the mono- (or double-) exponential expression $I = [(I_p - I_s)\, e^{-kt}] + I_s$ (or $I = [(I_p - I_i)\, e^{-k1t}] + [(I_i - I_s)\, e^{-k2t}] + I_s$, where I_i is the intermediate level of current and k_1 and k_2 are rate constants from the two separate decay processes). Curve fitting usually was done using data between 90 and 10% of the difference between peak and steady-state currents. The experimental data are presented as mean ± S.E., and comparisons of different conditions were analyzed for statistical significance using Student's *t* tests. All experiments were performed at room temperature (23 ± 1 °C). Dose-response profiles were fit to the Hill equation and analyzed using Origin 5.0.

Solutions and Drug Application—The standard external solution contained 120 mM NaCl, 3 mM KCl, 2 mM $MgCl_2$, 2 mM $CaCl_2$, 25 mM D-glucose, 10 mM HEPES, adjusted to pH 7.4 with Tris base. For conventional whole cell recordings, "$Tris^+$ electrodes" were used to prevent receptor functional run-down (37, 40), and were filled with solution containing 110 mM Tris phosphate dibasic, 28 mM Tris base, 11 mM EGTA, 2 mM $MgCl_2$, 0.1 mM $CaCl_2$, 4 mM Na-ATP, pH 7.3 (41). To initiate whole cell current responses, nicotinic agonists were delivered into the bath medium near the cell being recorded via a computer-controlled U-tube system so that solution exchange occurred within 20 ms (based on 10–90% peak current rise times). Intervals between drug applications (3 min) were adjusted specifically to ensure stability of nAChR responsiveness (without functional rundown). Drugs used in

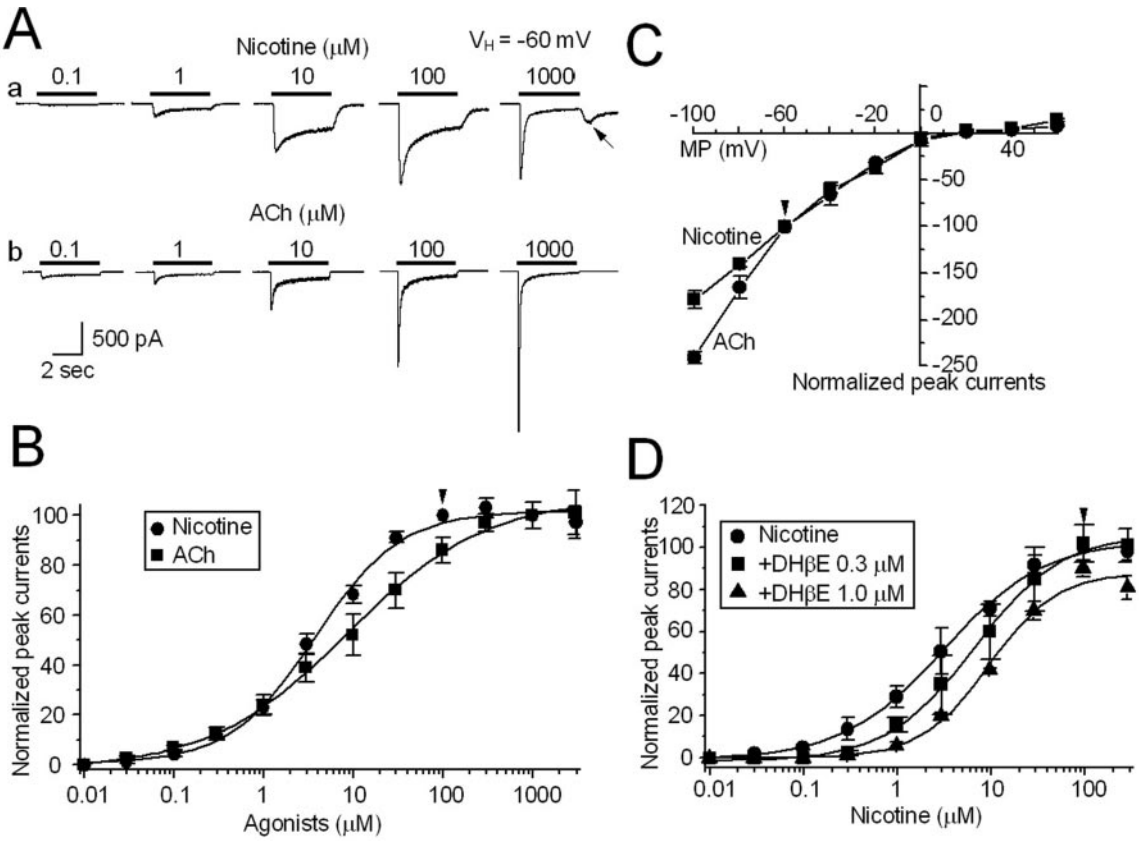

FIG. 2. **Basic functional properties of transfected human α4β2-nAChRs.** *A*, nicotine- and ACh-induced inward currents were obtained at different concentrations indicated along the *horizontal bars* showing the time course for drug application *above* each trace. At a high nicotine concentration (1 mM), washout of nicotine induced a rebound current (indicated by *arrow*). *B*, concentration-response relationship curves for nicotine and ACh. All *symbols* were normalized to current induced by 100 μM nicotine exposure (shown by the *arrowhead*). Each data point is the average from 6 to 8 cells tested, and the *vertical bars* indicate standard errors. *C*, 100 μM nicotine- and 1 mM ACh-induced inward currents at different holding potentials are superimposed. The current-voltage relationship curves for both nicotine and ACh responses show a clear inward rectification. All peak currents induced by agonists were normalized to the agonist responses at a holding potential of −60 mV (marked with the *arrowhead*). Each *symbol* is the average response from 7 to 8 cells. *D*, the sigmoidal nicotine concentration-peak current response curves in the absence or presence of 300 nM or 1 μM DHβE show that DHβE shifted the nicotine concentration-response curve to the right without affecting the maximal response, suggesting a competitive mechanism of antagonism. All symbols were normalized to the 100 μM nicotinic response (marked with the *arrowhead*), and each symbol is the average from 4 to 8 cells.

the present study were (−) nicotine, dihydro-β-erythroidine (DHβE), $A\beta_{40-1}$ (Sigma), and $A\beta_{1-42}$ (rPeptide, Athens, GA). Aβ peptides were reconstituted per vendor specifications in distilled water to a concentration of 100 μM, stored at −20 °C, and used within 10 days of reconstitution. Thawed peptide solutions and working dilutions in standard extracellular solution were used within 4 h before being discarded.

RESULTS

Heterologously Expressed hα4β2-nAChRs in SH-EP1 Cells—RT-PCR analysis confirmed expression of nAChR α4 and β2 subunit messages in SH-EP1-hα4β2 cells (Fig. 1*A*; α4β2). By contrast, whereas there was successful amplification of GAPDH message (positive control, *lane c*), no significant α4- or β2-specific product was observed in the host cell line (wild-type SH-EP1 cells). Results of *in situ* hybridization studies consistently found an absence of staining for nAChR α4 or β2 subunit messages reacting with sense or antisense riboprobes in untransfected SH-EP1 host cells (data not shown) or reacting with sense riboprobes in SH-EP1-hα4β2 cells (Fig. 1*B*, *a* and *b*). However, for reactions employing antisense riboprobes, nearly all SH-EP1-hα4β2 cells displayed strong perinuclear and cytoplasmic hybridization signals for both α4 and β2 subunits (Fig. 1, *B*, *a′* and *b′*), respectively. Furthermore, apparent levels of α4 or β2 subunit transcripts did not seem to fluctuate as a function of cell confluence or between grouped or solitary cells (data not shown). Immunoprecipitation-Western analyses using solubilized membrane samples from transfected SH-EP1-hα4β2 cells clearly indicated that α4 and β2 subunits are expressed as protein and assembled together (Fig. 1*C*). Finally, screening using whole cell current recordings confirmed that functional responses to 1 μM nicotine are evident in transfected SH-EP1-hα4β2 cells, but not in untransfected, wild-type SH-EP1 cells (Fig. 1*D*), indicating that transfected cells express functional hα4β2-nAChRs.

Basic Functional Properties of Transfected hα4β2-nAChRs—Whole cell current responses of heterologously expressed hα4β2-nAChRs show nicotine and acetylcholine (ACh) dose dependence (Fig. 2*A*) that translates into a sigmoid dose-response relationship characterized by a functional EC_{50} value for nicotine of 3.2 μM (Hill coefficient of 0.81) and for ACh of 9.2 μM (Hill coefficient of 0.6; Fig. 2*B*). Voltage dependence of hα4β2-nAChR responses to both nicotine and ACh (Fig. 2*B*) shows inward rectification at positive membrane potentials (Fig. 2*C*). Nicotine dose-response curves for hα4β2-nAChR-mediated currents obtained in the presence of 0.3 or 1 μM DHβE, which is a relatively selective antagonist of α4β2-nAChRs compared with other nAChR subtypes, are shifted to the right without showing an effect on peak whole cell current amplitude at maximal nicotine concentration (Fig. 2*D*). Compared with the EC_{50} value for nicotine alone (3.3 ± 0.6 μM, mean ± S.E. for separate EC_{50} measures from replicate experiments, $n = 10$), the EC_{50} obtained for nicotine in the presence of 300 nM DHβE is higher, but not significantly (4.7 ± 1.2 μM,

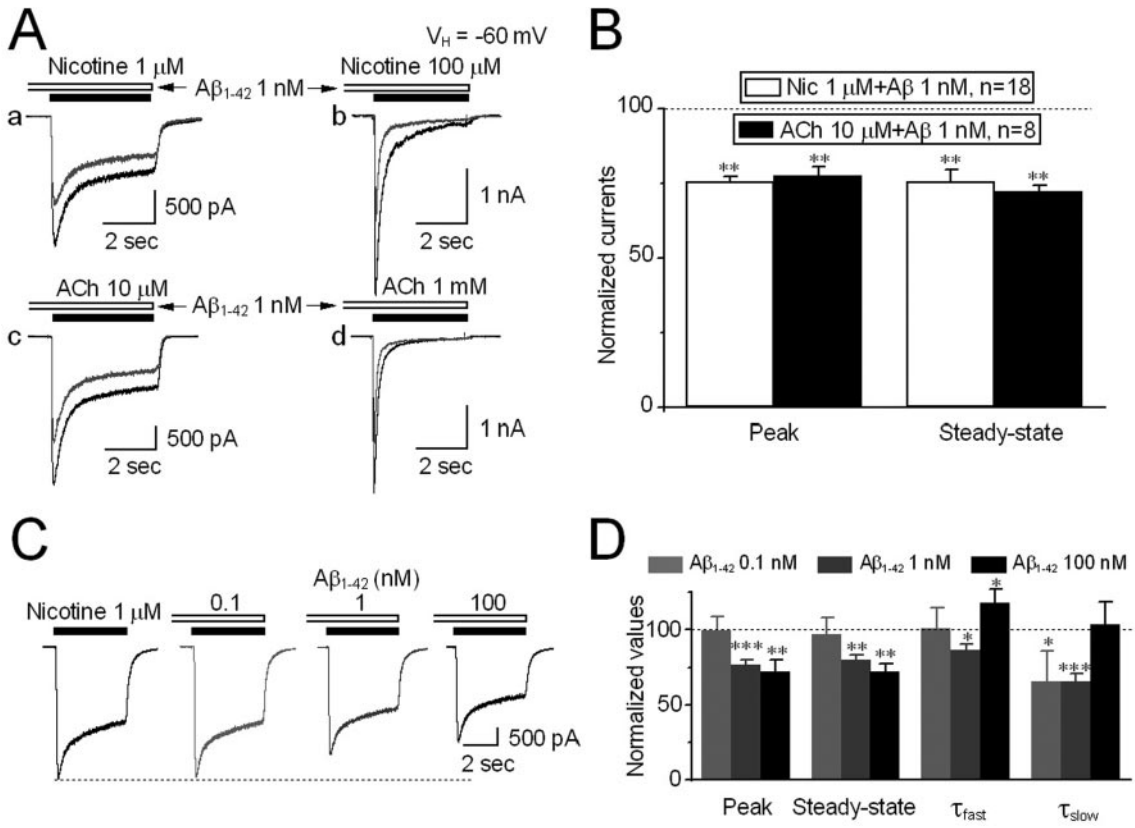

FIG. 3. **$A\beta_{1-42}$ acutely modulates human $\alpha4\beta2$-nAChR-mediated currents.** *A*, comparison of effects of 1 nM $A\beta_{1-42}$ on nicotine- and ACh-induced currents. Whole cell current response traces recorded from the same cell for *A* and *B*, and from another cell for *C* and *D*. *B*, *bar graph* summarizing results (peak and steady-state currents) from replicate studies. The *horizontal dashed line* indicates the control value (100%) for the specified parameter for the nicotinic response (induced by 1 μM nicotine and 10 μM ACh) before $A\beta_{1-42}$ treatment. *Double asterisk* means $p < 0.01$. *C* and *D*, concentration-dependent inhibition by $A\beta_{1-42}$ of h$\alpha4\beta2$-nAChR function induced by 1 μM nicotine is shown as individual traces recorded from the same cell (*C*), and results for the indicated parameters from replicate studies are summarized in *D*. In all recordings (*A* and *C*), the cells were held at a holding potential (V_H) of −60 mV. In *D*, the *asterisk* means $p < 0.05$, the *double asterisk* means $p < 0.01$, and the *triple asterisk* means $p < 0.001$. *Vertical bars* indicate standard errors.

$p > 0.05$, $n = 11$), but the EC_{50} obtained in the presence of nicotine plus 1 μM DHβE is significantly higher (9.6 ± 1.5 μM, $p < 0.05$, $n = 4$), but nicotine efficacy is not reduced in the presence of DHβE. Thus, DHβE exhibits features of competitive antagonism acting on heterologously expressed h$\alpha4\beta2$-nAChRs. These basic electrophysiological and pharmacological properties indicate that heterologously expressed h$\alpha4\beta2$-nAChRs in SH-EP1 cells exhibit characteristic features of the subtype and validate SH-EP1-h$\alpha4\beta2$ cells as models for studying h$\alpha4\beta2$-nAChR function.

$A\beta_{1-42}$ Acutely Inhibits h$\alpha4\beta2$-nAChR-mediated Whole Cell Currents—Initial studies done to examine the acute effects of 1 nM $A\beta_{1-42}$ on h$\alpha4\beta2$-nAChR responses to nicotine or ACh indicated that pretreatment (typically done for 3 min) with Aβ peptide was necessary to elicit a statistically significant, functional inhibition of peak current responses (reduced to 75.3 ± 2.1% of control values for nicotine, $n = 18$, $p < 0.01$; reduced to 77.4 ± 3.1% of control values for ACh, $n = 8$, $p < 0.01$; Fig. 3, *A* and *B*). $A\beta_{1-42}$ exposure also caused reduction of steady-state whole cell current responses to nicotine (reduced to 75.5 ± 2.2% of control values, $n = 18$, $p < 0.01$) or ACh (reduced to 71.5 ± 4.2% of control values, $n = 8$, $p < 0.01$; Fig. 3, *A* and *B*). Increases in rates and extents of acute desensitization, assessed as time constants for inward current decay from peak to steady-state levels and as the magnitude of the steady-state inward current, were evident for $A\beta_{1-42}$ action on h$\alpha4\beta2$-nAChRs responding to nicotine or ACh (Fig. 3*A, traces*). Because there were no differences in effects of $A\beta_{1-42}$ on ACh- or nicotine-induced h$\alpha4\beta2$-nAChR function, the remainder of the studies focused on the use of nicotine as the prototypical nicotinic agonist. Interestingly, without pretreatment, 1 nM $A\beta_{1-42}$ did not show significant reduction of peak current responses to nicotine (decreased to 94.3 ± 2.9% of control values, $n = 17$, $p > 0.05$), but the peptide reduced steady-state currents to 76 ± 6.0% of control values ($n = 17$, $p < 0.01$; data not illustrated). Studies using the reverse-sequence peptide $A\beta_{40-1}$ failed to show significant inhibition of h$\alpha4\beta2$-nAChR function (data also not illustrated), suggesting that effects were peptide sequence-specific. An additional set of studies examining the effects of different concentrations of $A\beta_{1-42}$ on responses to 1 μM nicotine showed dose-dependence of h$\alpha4\beta2$-nAChR functional block (Fig. 3, *C* and *D*). Collectively, these results indicate that $A\beta_{1-42}$ acutely inhibits h$\alpha4\beta2$-nAChR function.

Possible Mechanisms Involved in $A\beta_{1-42}$ Inhibition of h$\alpha4\beta2$-nAChR Function—Dose-response profiles of nicotine-induced whole cell peak currents in the absence or presence of 1 nM $A\beta_{1-42}$ showed similar magnitudes of peptide-induced functional inhibition and no dramatic change in nicotine EC_{50} values or Hill coefficients (3.3 ± 0.6 and 0.97 ± 0.07 μM, respectively, for nicotine alone, $n = 10$; 4.1 ± 0.9 and 1.1 ± 0.1 μM, respectively, for nicotine plus 1 nM $A\beta_{1-42}$, $n = 5$, $p > 0.05$), suggesting a non-competitive mechanism of inhibition (Fig. 4, *A* and *B*). Other studies indicated that 1 nM $A\beta_{1-42}$ showed similar inhibition of 100 μM nicotinic-induced responses at different holding potentials (V_H), suggesting a voltage-independent means of functional inhibition by $A\beta_{1-42}$ (Fig. 4, *C* and *D*). A repeated application protocol with nicotine in the continuous presence of 1 nM $A\beta_{1-42}$ demonstrated that 1 nM $A\beta_{1-42}$ did not

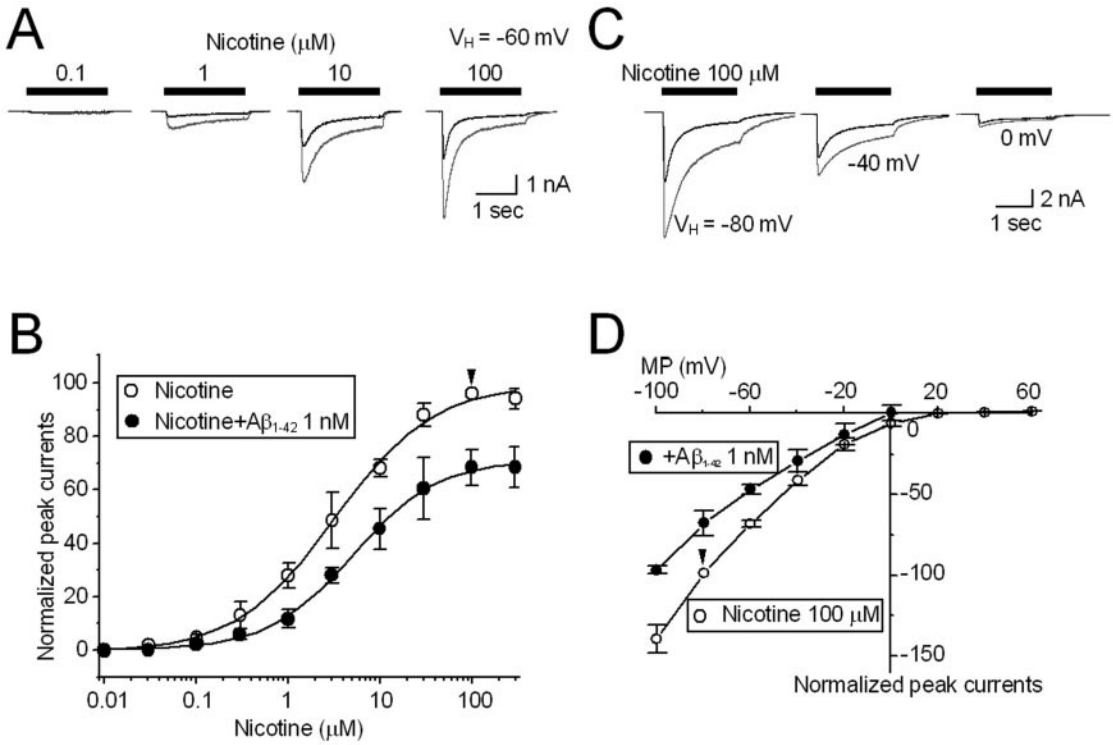

FIG. 4. **$A\beta_{1-42}$ inhibits human $\alpha4\beta2$-nAChR-mediated currents in a non-competitive and voltage-independent manner.** *A*, individual whole cell current traces for responses to nicotine at the indicated concentrations alone (higher amplitude traces) or in the presence of 1 nM $A\beta_{1-42}$ (smaller amplitude traces). *B*, results of replicate studies (as in *A*) fit to the logistic equation indicate a downward shift reflecting reduction of maximal current response in the agonist dose-response profile in the presence of $A\beta_{1-42}$, but without a change in apparent EC_{50} for agonist, characteristic of non-competitive inhibition. All *symbols* were normalized to the peak current induced by 100 μM nicotine (marked by the *arrowhead*), and each symbol is the average from 10 cells for nicotine, and 5 cells for nicotine plus 1 nM $A\beta_{1-42}$. *C*, representative whole cell current traces in response to 100 μM nicotine alone (higher amplitude traces) or in the presence of 1 nM $A\beta_{1-42}$ (lower amplitude traces) at different holding potentials as indicated. *D*, plots of whole cell peak current amplitude as a function of holding potentials. All symbols were normalized to nicotine-induced peak current at a V_H of −80 mV (marked by the *arrowhead*) and are averages of recordings from 5 to 6 cells. *Vertical bars* indicate standard errors.

show clear signs of use-dependent inhibition of hα4β2-nAChRs (Fig. 5, *A* and *C*). Interestingly, after 15 min of continuous exposure to 1 nM $A\beta_{1-42}$ followed by peptide washout for 6 min, peak current responses to nicotine did not recover fully (Fig. 5, *A* and *C*). The absence of use-dependence suggests that non-competitive inhibition of hα4β2-nAChR function by $A\beta_{1-42}$ is not mediated through open channel block, although the persistence in functional block after washout of fluid phase Aβ suggests a lingering effect of the peptide (see "Discussion"). To address whether $A\beta_{1-42}$-induced hα4β2-nAChR internalization is involved in this incomplete functional recovery after relatively long term exposure (15 min) of hα4β2-nAChRs to 1 nM $A\beta_{1-42}$, we pre-loaded recorded cells with GDPβS (600 μM) for 20 min, which was reported to prevent α-amino-3-hydroxy-5-methyl-4-isoxazolepropionate receptor endocytosis (42), and we repeated the experiment shown in Fig. 5*A*. GDPβS treatment neither prevented $A\beta_{1-42}$-mediated inhibition, nor improved hα4β2-nAChR functional recovery from washout of $A\beta_{1-42}$ (Fig. 5, *B* and *C*), suggesting that the inhibition of hα4β2-nAChR function by $A\beta_{1-42}$ is not mediated via hα4β2-nAChR internalization through the process affecting α-amino-3-hydroxy-5-methyl-4-isoxazolepropionate receptors.

Acceleration of hα4β2-nAChR Acute Desensitization by $A\beta_{1-42}$ Is Not Influenced by β2 Subunit Intracellular Domains—The data presented thus far indicate that 1 nM $A\beta_{1-42}$ accelerates hα4β2-nAChR desensitization. We considered whether this modulation could be via mechanisms involving sequences in the nAChR β2 subunit large, cytoplasmic loop that are potentially involved in nAChR phosphorylation (46), possibly engaged in coupling to the cytoskeleton or cytoplasmic modulators, or perhaps involved in some other intracellular mechanism mediating $A\beta_{1-42}$ action. To test these possibilities, we created chimeric β2 (β2ch) subunits whose natural cytoplasmic loop sequences were replaced by those from the mouse serotonin receptor 5-TH_{3A} subunit sequence. α4β2ch-nAChR-mediated currents showed significant acceleration of receptor desensitization compared with rates of desensitization for fully wild-type α4β2-nAChRs (Fig. 6, *A* and *B*). However, 1 nM $A\beta_{1-42}$ further accelerated receptor desensitization and lowered peak and steady-state components of nicotine-induced whole cell currents in either α4β2- or α4β2ch-nAChRs (Fig. 6, *C* and *D*). These results suggest that accelerated α4β2-nAChR desensitization upon $A\beta_{1-42}$ exposure is not influenced by changes in the nAChR β2 subunit cytoplasmic loop sequence.

Selective Inhibition of hα4β2-nAChR Function at Pathophysiologically Relevant Concentrations of $A\beta_{1-42}$—Given reports of interactions at high concentrations (100–3000 nM) of $A\beta_{1-42}$ with α7-nAChRs (22, 23, 25, 26) and rat α4β2-nAChRs (24), we compared effects of $A\beta_{1-42}$ on function of heterologously expressed hα4β2-nAChRs to effects on heterologously expressed hα7-nAChRs expressed in the same cellular host (40). $A\beta_{1-42}$, at a pathophysiologically relevant concentration (1 nM), clearly inhibits nicotinic peak current responses mediated by hα4β2-nAChRs (inhibition to 76% of control values; Fig. 7*A*, *left*), but not responses mediated by hα7-nAChRs (Fig. 7*B*, *left*). However, at a higher concentration (100 nM), $A\beta_{1-42}$ inhibits both hα4β2-nAChR- (to 68% of control values; Fig. 7*A*, *right*) and hα7-nAChR-mediated peak currents (to 41% of control values; Fig. 7*B*, *right*), although the magnitude of functional inhibition of α7-nAChRs is greater. Interestingly, the

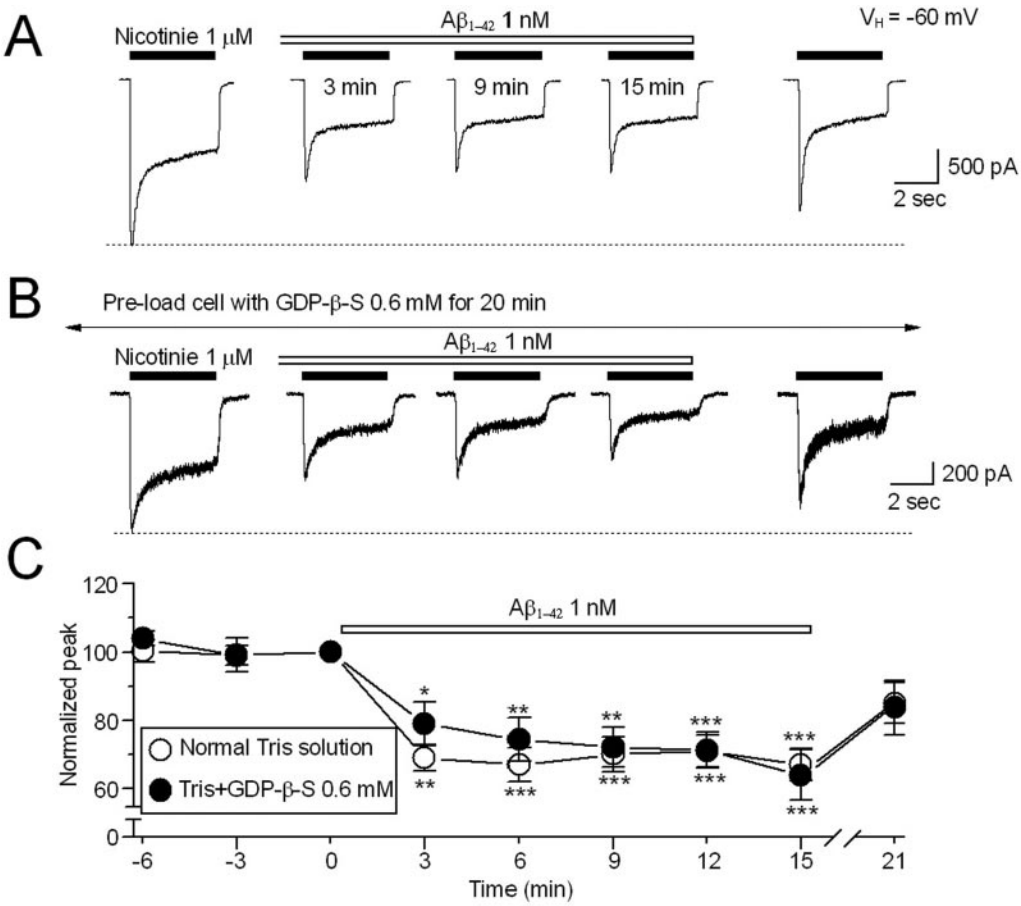

FIG. 5. **Mechanisms involved in Aβ_{1-42} inhibition of human $\alpha4\beta2$-nAChR-mediated currents.** *A*, representative whole cell current traces recorded using normal Tris solution-filled pipettes. 1 μM nicotine was repetitively applied (4-s exposure at an interval of 3 min). The first three responses were recorded as controls, then nicotine exposures were repeated at 3-min intervals in the continuous presence of 1 nM Aβ_{1-42} for 15 min, and then an additional response to nicotine was recorded after 6 min of washout of Aβ_{1-42}. *B*, representative whole cell current traces recorded using Tris-filled pipettes supplemented with 600 μM GDPβS. Initial responses to nicotine were measured after 20 min of intracellular GDPβS exposure, and the sequence of drug applications was as described in *A*. *C*, temporal patterns show the similar effects of 1 nM Aβ_{1-42} on nicotinic responses with and without GDPβS in the pipette solution. The *asterisk* means $p < 0.05$, the *double asterisk* means $p < 0.01$, and the *triple asterisk* means $p < 0.001$. *Vertical bars* indicate standard errors.

inhibition of h$\alpha4\beta2$-nAChR-mediated currents by 1 or 100 nM Aβ_{1-42} appears to occur through different mechanisms because 1 nM Aβ_{1-42} accelerated the rate of current decay from peak to steady-state levels without changing the half-time for achievement of peak currents, whereas 100 nM Aβ_{1-42} slowed current rising time without changing decay time (Figs. 3*D* and 7, *A* and *C*). Nevertheless, these results indicate that heterologously expressed h$\alpha4\beta2$-nAChRs are more sensitive than h$\alpha7$-nAChRs to pathophysiologically relevant concentrations (1 nM) of Aβ_{1-42}.

DISCUSSION

Principal Observations—These studies validate SH-EP1-h$\alpha4\beta2$ cells as a model for investigation of the properties of h$\alpha4\beta2$-nAChRs. The cells express nAChR $\alpha4$ and $\beta2$ subunits as mRNAs and receptor subunit proteins that co-assemble to yield nAChRs that show functional responses to nicotine or ACh that are sensitive to competitive inhibition by DHβE and that are manifest as inwardly rectifying whole cell currents on patch clamp analysis. Aβ_{1-42} peptides, but not control Aβ_{40-1} peptides, inhibit function of h$\alpha4\beta2$-nAChRs at concentrations as low as 1 nM. Effects are manifest as a reduction in whole cell peak and steady-state currents and acceleration of rates of desensitization. Effects show no use-dependence or voltage-dependence and persist after bulk removal of peptide in solution. Features of functional inhibition are the same for $\alpha4\beta2$-nAChRs and nAChRs composed of $\alpha4$ subunits and a chimeric form of $\beta2$ subunits containing alternate cytoplasmic loop amino acids. Aβ_{1-42}-mediated inhibition of human $\alpha7$-nAChR function also is observed, but at higher concentrations (100 nM).

nAChR Subtype Selectivity of Aβ Effects and Effective Doses—When we began these studies, there were some points of controversy in the earlier literature concerning Aβ/nAChR interactions. Liu *et al.* (23) reported that 100 nM Aβ_{1-42} suppressed $\alpha7$-nAChR-mediated currents but failed to block peak whole cell current responses attributed to non-$\alpha7$-nAChRs expressed on cultured rat hippocampal neurons. By contrast, Pettit *et al.* (22) found that 2 μM Aβ_{1-42} inhibited single channel opening probability of both $\alpha7$- (38 pS channel; by 14%) and, more potently, non-$\alpha7$- (62 pS channel, by 54%) nAChR-mediated currents recorded from excised membrane patches derived from rat hippocampal slices. Although the non-$\alpha7$-nAChR subtypes studied by Liu *et al.* (23) and Pettit *et al.* (24) were not specifically identified, studies of heterologously expressed rat $\alpha4\beta2$-nAChRs in *Xenopus* oocytes revealed that 10-min pretreatment with 100 nM Aβ_{1-42} depressed peak whole cell currents to 62% of control levels while having a much smaller effect on rat $\alpha7$-nAChRs (24). Heterologously expressed (in oocytes) human (25) or rat (26) $\alpha7$-nAChRs are functionally blocked by preincubation with 100 nM Aβ_{1-42}. However, oocyte-expressed rat $\alpha7$-nAChR responses are reported to be activated by the initial application of 1–100 pM Aβ_{1-42} (26). Other studies using acutely dissociated, rat basal forebrain neurons indicated

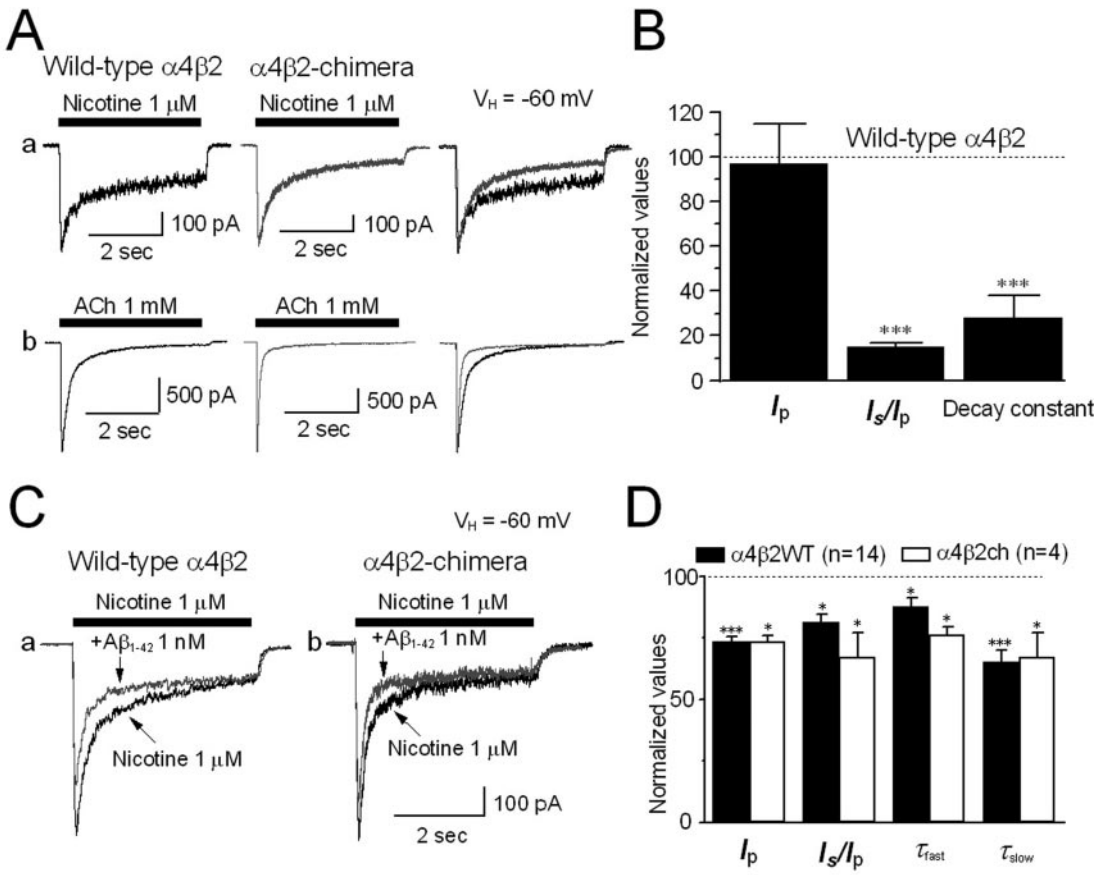

FIG. 6. **$A\beta_{1-42}$ inhibits both wild-type h$\alpha4\beta2$-nAChR- and h$\alpha4\beta2$-chimera-nAChR-mediated currents.** *A*, representative whole cell current traces for responses to 1 μM nicotine (*a*) or 1 mM ACh (*b*) of fully wild-type hα4β2-nAChRs and nAChRs containing wild-type α4 and chimeric β2 subunits (α4β2-chimera). *Right panels* superimpose the nicotinic responses from the *left* and *middle panels*. *B*, *bar graphs* compare 1 μM nicotine-induced whole cell currents recorded from transfected wild-type hα4β2-nAChRs and α4β2-chimera-nAChRs. The normalized wild-type hα4β2-nAChR-mediated currents (as 100%) are presented as a *horizontal dashed line*. I_p and I_s mean the peak and steady-state currents, respectively. *C*, representative whole cell current traces for responses to 1 μM nicotine alone or in the presence of 1 nM $A\beta_{1-42}$ (lower amplitude traces) for wild-type hα4β2-nAChRs (*a*) or for α4β2-chimera-nAChRs (*b*). *D*, summary of effects of 1 nM $A\beta_{1-42}$ on peak and steady-state current amplitudes and on fast and slow phases of nAChR desensitization in 4–14 replicate studies. The *asterisk* means $p < 0.05$ and the *triple asterisk* means $p < 0.001$. *Vertical bars* indicate standard errors.

that 4 μM $A\beta_{25-35}$ or 100 nM $A\beta_{1-42}$ directly activated single channels and that 10 or 100 nM $A\beta_{1-42}$ induced whole cell current responses attributable to a non-α7-nAChR subtype (likely α4β2-nAChR), also suggesting agonist-like activity of Aβ on nAChRs (43). Our observations showing (for the first time) significant functional inhibition of hα4β2-nAChRs by 1 nM $A\beta_{1-42}$ and finding (consistent with cross-species observations) (22–26) inhibition of hα7-nAChRs by 100 nM $A\beta_{1-42}$ indicate that $A\beta_{1-42}$ acts as a nAChR functional antagonist with higher affinity for hα4β2-nAChRs than for hα7-nAChRs. Doses at which confirmed, high affinity, nicotine-binding hα4β2-nAChRs are affected by $A\beta_{1-42}$ are in the range of peptide concentrations of potential pathological relevance, *i.e.* similar to those (0.01–5 nM) found in AD patient cerebrospinal fluid (44, 45).

Possible Mechanisms of $A\beta_{1-42}$-mediated Inhibition of hα4β2-nAChR Function—The present results clearly support the hypothesis that Aβ directly modulates nAChR function. Our data shows that $A\beta_{1-42}$, at concentrations from 1 pM to 1 μM, failed to directly induce whole cell current responses from cells expressing hα4β2- or hα7-nAChRs or from untransfected cells, meaning that Aβ, in our hands, and although signal transduction through other means remains a possibility, does not have properties of a nAChR agonist able to induce whole cell currents. This finding is in agreement with previous reports that $A\beta_{1-42}$ failed to elicit naturally expressed α7-nAChR-mediated currents in cultured hippocampal neurons (23) or heterologously expressed α7-nAChR responses in *Xenopus* oocytes (25), but it is not consistent with $A\beta_{1-42}$ binding to rat α7- or non-α7-nAChRs (likely α4β2-nAChRs) at an agonist, co-agonist, or other allosteric, positive modulatory site involved in eliciting or enhancing whole cell currents (26, 43). Agonism (or competitive antagonism) also is inconsistent with our repeated findings[2] failing to detect direct competition of picomolar to micromolar $A\beta_{1-42}$ with radioligand binding sites on heterologously expressed hα4β2- or hα7-nAChRs. On the contrary, our findings indicate that $A\beta_{1-42}$ acts as a non-competitive antagonist of hα4β2-nAChRs under our experimental conditions. A non-competitive mechanism of naturally or heterologously expressed α7-nAChR functional block by $A\beta_{1-42}$ also has been invoked (22, 25).

As to the domain(s) involved in non-competitive block, our data indicating that effects of $A\beta_{1-42}$ on hα4β2-nAChR function are not affected by changes in amino acid sequences corresponding to the β2 subunit second, major intracellular domain, suggests an alternate site of action. Other chimera studies of α7-nAChRs more directly indicated a role for the NH_2-terminal extracellular domain of the α7 subunit in Aβ effects on that subtype (23). Our data showing no use or voltage dependence of $A\beta_{1-42}$ inhibition of hα4β2-nAChR function suggests that effects are not mediated via open channel block. In

[2] S. Morrissy, L. H. Wilkins, Jr., K. M. Schroeder, and R. J. Lukas, unpublished data.

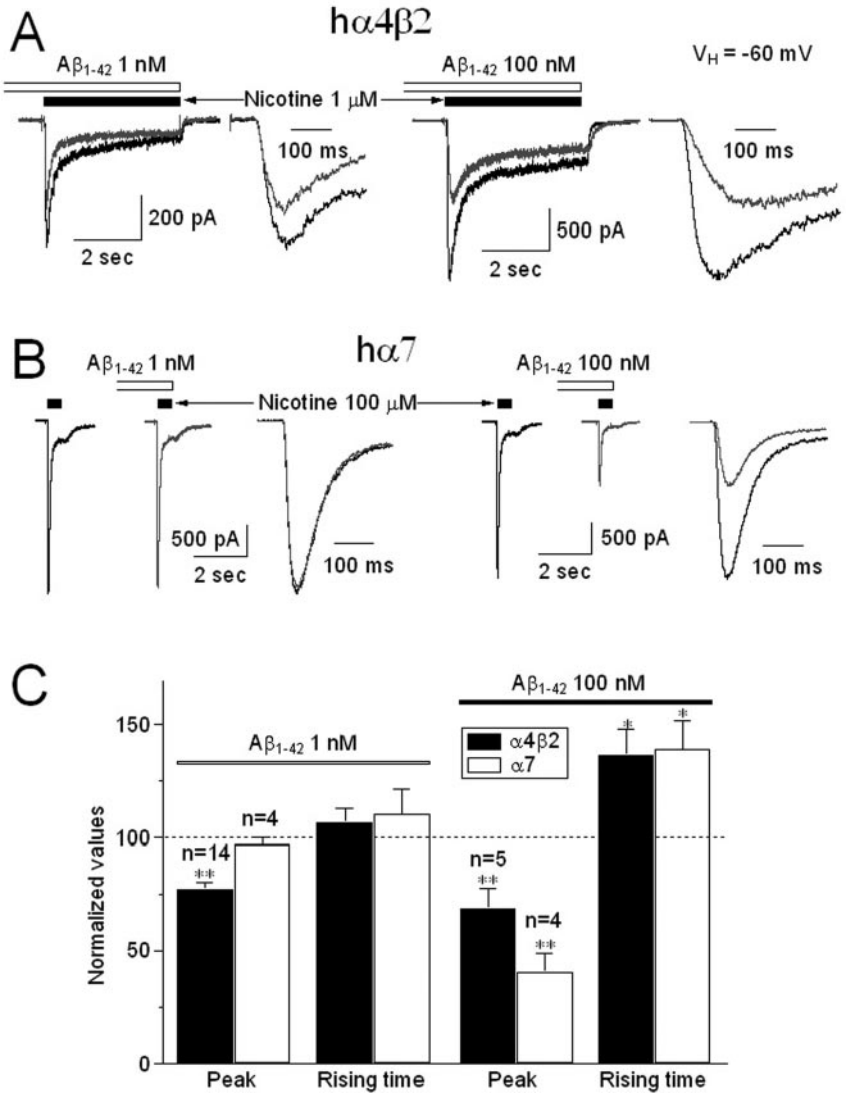

FIG. 7. **1 nM $A\beta_{1-42}$ selectively inhibits human $\alpha4\beta2$- but not human $\alpha7$-nAChR-mediated currents.** *A*, representative whole cell current traces comparing effects of 1 nM (*left*) and 100 nM (*right*) $A\beta_{1-42}$ on function of $\alpha4\beta2$-nAChRs showing functional inhibition of comparable magnitude at both concentrations, but slower activation (rising time) kinetics in the presence of 100 nM peptide. Note the different time scales in the pairs of traces allowing for clearer resolution of rising phases in the *right-hand traces*. *B*, representative whole cell current traces comparing effects of 1 (*left*) and 100 nM (*right*) $A\beta_{1-42}$ on function of $\alpha7$-nAChRs showing functional inhibition only at 100 nM. Note the different time scales in the pairs of traces allowing for clearer resolution of rising phases in the *right-hand traces*. *C*, *bar graph* summarizing observations of effects of 1 or 100 nM $A\beta_{1-42}$ on the peak component and rising time to peak current for responses mediated by human $\alpha4\beta2$-nAChRs (*filled bars*) or $\alpha7$-nAChRs (*open bars*). The *asterisk* means $p < 0.05$ and the *double asterisk* means $p < 0.01$. *Vertical bars* indicate standard errors.

agreement with other studies (23–26), we also found that pretreatment with $A\beta_{1-42}$ is necessary to induce convincing inhibition of $h\alpha4\beta2$-nAChR-mediated nicotinic responses. The nature of this slow onset of inhibition is still unknown, although it has been hypothesized that $A\beta_{1-42}$ may drive nAChRs into a long-lived closed conformation. This hypothesis is supported by the present observation that long exposure (15 min) to $A\beta_{1-42}$ led to persistent loss of $h\alpha4\beta2$-nAChR function, although any loss of nAChR function does not seem to be mediated via $A\beta_{1-42}$-induced $h\alpha4\beta2$-nAChR internalization. Our finding that $A\beta_{1-42}$ exposure accelerated rates of $h\alpha4\beta2$-nAChR functional desensitization is consistent with another report that $A\beta_{1-42}$ accelerated the rate of current decay for muscle-type nAChRs (25). A possible role of changes in nAChR phosphorylation state in regulation of receptor desensitization has been proposed (46), but our studies suggest that any such role for $h\alpha4\beta2$-nAChR phosphorylation would be because of changes in $\alpha4$ subunit phosphorylation state.

Pathological Relevance of $\alpha4\beta2$-nAChR Dysfunction and AD—nAChRs that bind radiolabeled nicotine with the highest affinity contain $\alpha4$ subunits ($\alpha4$*-nAChR; for review, see Refs. 47–51). Immunoassays have shown that the predominant, naturally expressed form of the $\alpha4$*-nAChR in the vertebrate brain contains $\alpha4$ and $\beta2$ subunits ($\alpha4\beta2$-nAChR) (17, 18). Evidence indicates that a consistent, significant loss of $\alpha4$*-nAChRs has been observed at autopsy in a number of neocortical areas and hippocampi of patients with AD (for reviews, see Refs. 52 and 53). Cortical $\alpha4$*-nAChR deficits are significantly correlated with cognitive impairment in AD patients (54, 55). The major pathological features of AD are Aβ protein deposition and a severe cholinergic deficit. It has been shown that Aβ protein serves as a major constituent of senile plaques, a neuropathologic hallmark of AD and a neurotoxin through *in vivo* and *in vitro* studies. $A\beta_{1-42}$ accumulation and aggregation are thought to contribute to the pathology of AD. However, links between soluble $A\beta_{1-42}$ elevation and cholinergic dysfunction remain unclear. The present studies provide the basis for a new hypothesis that $A\beta_{1-42}$-induced $h\alpha4\beta2$-nAChR functional depression may contribute to cholinergic signaling deficits and/or neurodegeneration that are hallmarks of AD. This hypothesis is not necessarily exclusive of, for example, other mechanisms that would produce selective death of cholinergic neurons, would result in destabilization of membrane properties by Aβ and/or its precursors (56–59), or would reflect effects of Aβ on intracellular Ca^{2+} homeostasis through either production of cation ionophores or activation of ligand- and/or voltage-gated channels (60, 61). Our perspective on a primary role for $h\alpha4\beta2$-nAChRs in low concentration effects of Aβ complements other suggestions that the modulation of nAChR function by Aβ could be pathologically relevant (20–26, 43).

In conclusion, this study provides evidence for a possible link between abnormal deposits of $A\beta_{1-42}$ and $h\alpha4\beta2$-nAChR dys-

function in AD patients. Furthermore, the finding that human α4β2-nAChRs are sensitive targets of pathophysiologically relevant concentrations of $A\beta_{1-42}$ suggests novel strategies for AD therapy that would involve amelioration of peptide-induced α4β2-nAChR functional block and/or perhaps preservation of α4β2-nAChR activity.

Acknowledgment—We thank J. Brek Eaton for maintenance of SH-EP1-hα4β2 cells.

REFERENCES

1. Prince, D. L., and Sisodia, S. S. (1998) *Annu. Rev. Neurosci.* **21,** 479–505
2. Selkoe, D. J. (2000) *Ann. N. Y. Acad. Sci.* **924,** 17–25
3. Auld, D. S., Kar, S., and Quirion, R. (1998) *Trends Neurosci.* **21,** 43–49
4. Kar, S., Seto, D., Gaudreau, P., and Quirion, R. (1996) *J. Neurosci.* **16,** 1034–1040
5. Kelly, J. F., Furukawa, K., Barger, S. W., Rengen, M. R., Mark, R. J., Blanc, E. M., Roth, G. S., and Mattson, M. P. (1996) *Proc. Natl. Acad. Sci. U. S. A.* **93,** 6753–6758
6. Pedersen, W. A., Kloczewiak, M. A., and Blusztajn, J. K. (1996) *Proc. Natl. Acad. Sci. U. S. A.* **93,** 8068–8071
7. Galdzicki, Z., Fukuyama, R., Wadhwani, K. C., Rapoport, S. I., and Ehrenstein, G. (1994) *Brain Res.* **646,** 332–336
8. Hoshi, M., Takashima, A., Murayama, M., Yasutake, K., Yoshida, N., Ishiguro, K., Hoshino, T., and Imahori, K. (1997) *J. Biol. Chem.* **272,** 2038–2041
9. Hoshi, M., Takashima, A., Noguchi, K., Murayama, M., Sato, M., Kondo, S., Saitoh, Y., Ishiguro, K., Hoshino, T., and Imahori, K. (1997) *Proc. Natl. Acad. Sci. U. S. A.* **93,** 2719–2723
10. Mark, R. J., Pang, Z., Geddes, J. W., Uchida, K., and Mattson, M. P. (1997) *J. Neurosci.* **17,** 1046–1054
11. Kamenetz, F., Tomita, T., Hsieh, H., Seabrook, G., Borchelt, D., Iwatsubo, T., Sisodia, S., and Malinow, R. (2003) *Neuron* **37,** 925–937
12. Paterson, D., and Noreberg, A. (2000) *Prog. Neurobiol.* **61,** 75–111
13. Warpman, U., and Nordberg, A. (1995) *Neuroreport* **6,** 2419–2423
14. Martin-Ruiz, C. M., Court, J. A., Molnar, E., Lee, M., Gotti, C., Mamalaki, A., Tsouloufis, T., Tzartos, S., Ballard, C., Perry, R. H., and Perry, E. K. (1999) *J. Neurochem.* **73,** 1635–1640
15. Nordberg, A., Hartvig, P., Lilja, A., Vitanen, M., Amberla, K., and Lundqvist, H. (1990) *J. Neurol. Transm.* **2,** 215–224
16. Rezvani, A. H., and Levin, E. D. (2001) *Biol. Psychiatry* **49,** 258–267
17. Whiting, P. J., and Lindstrom, J. (1987) *Proc. Natl. Acad. Sci. U. S. A.* **84,** 595–599
18. Flores, C. M., Rogers, S. W., Pabreza, L. A., Wolfe, B. B., and Kellar, K. J. (1992) *Mol. Pharmacol.* **41,** 31–37
19. Sparks, D. L., Beach, T., and Lukas, R. J. (1998) *Neurosci. Lett.* **256,** 151–154
20. Wang, H. Y., Lee, D. H. S., D'Andrea, M. R., Peterson, P. A., Shank, R. P., and Beitz, A. B. (2000) *J. Biol. Chem.* **275,** 5626–5632
21. Wang, H. Y., Lee, D. H. S., Davis, C. B., and Shank, R. P. (2000) *J. Neurochem.* **75,** 1155–1161
22. Pettit, D. L., Shao, Z., and Yakel, J. L. (2001) *J. Neurosci.* **21,** 1–5
23. Liu, Q-S., Kawai, H., and Berg, D. K. (2001) *Proc. Natl. Acad. Sci. U. S. A.* **98,** 4734–4739
24. Tozaki, H., Matsumoto, A., Kanno, T., Nagai, K., Yamamoto, S., and Nishizaki, T. (2002) *Biochem. Biophys. Res. Commun.* **294,** 42–45
25. Grassi, F., Palma, E., Tonini, R., Amici, M., Ballivet, V., and Eusebi, F. (2003) *J. Physiol.* **547,** 147–157
26. Dineley, K. T., Bell, K., Bui, D., and Sweatt, J. D. (2002) *J. Biol. Chem.* **277,** 25056–25061
27. Picciotto, M. R., Zoli, M., Lena, C., Bessis, A., Lallemand, Y., Le Novere, N., Vincent, P., Pich, E. M., Brulet, P., and Changeux, J. P. (1995) *Nature* **374,** 65–67
28. Marubio, L. M., Gardier, A. M., Durier, S., David, D., Klink, R., Arroyo-Jimenez, M. M., McIntosh, J. M., Rossi, F., Champtiaux, N., Zoli, M., and Changeux, J. P. (2003) *Eur. J. Neurosci.* **17,** 1329–1337
29. Newhouse, P. A., Potter, A., Kelton, M., and Corwin, J. (2001) *Biol. Psychiatry* **49,** 268–278
30. Maelicke, A., Samochocki, M., Fehrenbacher, A., Ludwig, J., Albuquerque, E. X., and Zerlin, M. (2001) *Biol. Psychiatry* **49,** 279–288
31. Coyle, J., and Kershaw, P. (2001) *Biol. Psychiatry* **49,** 289–299
32. Puchacz, E., Buisson, B., Bertrand, D., and Lukas, R. J. (1994) *FEBS Lett.* **354,** 155–159
33. Peng, J.-H., Lucero, L., Fryer, J., Herl, J., Leonard, S. S., and Lukas, R. J. (1999) *Brain Res.* **825,** 172–179
34. Eaton, J. B., Peng, J. H., Schroeder, K. M., George, A. A., Fryer, J. D., Krishnan, C., Buhlman, L., Kuo, Y. P., Steinlein, O., and Lukas, R. J. (2003) *Mol. Pharmacol.* **64,** 1283–1294
35. Lukas, R. J., Norman, S. A., and Lucero, L. (1993) *Mol. Cell. Neurosci.* **4,** 1–12
36. Bencherif, M., and Lukas, R. J. (1993) *J. Neurochem.* **61,** 852–864
37. Kuo, Y.-P., Wu, J., Zhao, L., Xu, L., and Lukas, R. J. (2002) *Soc. Neurosci. Abst.* **28,** 537.13
38. Wu, J., Harata, N., and Akaike, N. (1996) *Br. J. Pharmacol.* **119,** 1013–1021
39. Wu, J., Chan, P., Schroeder, K. M., Ellsworth, K., and Partridge, L. D. (2002) *J. Neurochem.* **83,** 87–99
40. Zhao, L., Kuo, Y. P., George, A. A., Peng, J. H., Purandare, M. S., Schroeder, K. M., Lukas, R. J., and Wu, J. (2003) *J. Pharmacol. Exp. Ther.* **305,** 1132–1141
41. Huguenard, J. G., and Prince, D. A. (1994) *J. Neurosci.* **12,** 3804–3817
42. Lüscher, C., Xia, H., Beattie, E. C., Carroll, R. C., von Zastrow, M., Malenka, R. C., and Nicoll, R. A. (1999) *Neuron* **24,** 649–658
43. Fu, W., and Jhamandas, J. H. (2003) *J. Neurophysiol.* **90,** 3130–3136
44. Mehta, P. D., Pirttila, T., Mehta, S. P., Sersen, E. A., Aisen, P. S., and Wisniewski, H. M. (2000) *Arch. Neurol.* **57,** 100–105
45. Kuo, Y.-M., Kokjohn, T. A., Kalback, W., Luehrs, D., Galasko, D. R., Chevallier, N., Koo, E. H., Emmerling, M. R., and Roher, A. E. (2000) *Biochem. Biophys. Res. Commun.* **268,** 750–756
46. Huganir, R. L., and Greengard, P. (1990) *Neuron* **5,** 555–567
47. Lukas, R. J. (1998) in *Neuronal Nicotinic Acetylcholine Receptors: The Nicotinic Acetylcholine Receptor: Current Views and Future Trends* (Barrantes, F. J., ed) pp. 145–173, Springer-Verlag, Berlin and RG Landes Co., Georgetown, TX
48. Lukas, R. J., Albuquerque, E. X., Balfour, D. J. K., Clarke, P. B. S., Lindstrom, J. M., Novère, N., Le Quik, M., and Wonnacott, S. (2000) *Nicotinic Acetylcholine Receptors: The IUPHAR Compedium of Receptor Characterization and Classification*, IUPHAR Media, London
49. Lukas, R. J., Changeux, J. P., Le Novere, N., Albuquerque, E. X., Balfour, D. J., Berg, D. K., Bertrand, D., Chiappinelli, V. A., Clarke, P. B., Collins, A. C., Dani, J. A., Grady, S. R., Kellar, K. J., Lindstrom, J. M., Marks, M. J., Quik, M., Taylor, P. W., and Wonnacot, S. (1999) *Pharmacol. Rev.* **51,** 397–401
50. Lindstrom, J. (1996) in *Ion Channels* (Narahashi, T., ed) Vol. 4, pp. 377–450, Plenum Press, NY
51. Alexander, S. P. H., and Peters, J. A. (eds) (2001) *Trends in Pharmacological Science, Receptor Ion* Channel Nomenclature Supplement, Elsevier, London
52. Court, J., Martin-Ruiz, C., Piggott, M., Spurden, D., Griffiths, M., and Perry, E. (2001) *Biol. Psychiatry* **49,** 175–184
53. Nordberg, A. (2001) *Biol. Psychiatry* **49,** 200–210
54. Nordberg, A., Lundqvist, H., Hartvig, P., Lilja, A., and Langstrom, B. (1995) *Alzheimer Dis. Assoc. Disord.* **9,** 21–27
55. Nordberg, A., Lundqvist, H., Hartvig, P., Andersson, J., Johansson, M., Hellstrom-Lindahi, E., and Langstrom, B. (1997) *Dement. Geriatar. Cogn. Disord.* **8,** 78–84
56. Avdulov, N. A., Chochina, S. V., Igbavboa, U., O'Hare, E. O., Schroeder, F., Cleary, J. P., and Wood, W. G. (1997) *J. Neurochem.* **68,** 2086–2091
57. Muller, W. E., Koch, S., Eckert, A., Hartmann, H., and Scheuer, K. (1995) *Brain Res.* **674,** 133–136
58. Kanfer, J. N., Sorrentino, G., and Sitar, D. S. (1999) *Neurochem. Res.* **24,** 1621–1630
59. Fenster, C. P., Beckman, M. L., Parker, J. C., Sheffield, E. B., Whitworth, T. L., Quick, M. W., and Lester, R. A. (1999) *Mol. Pharmacol.* **55,** 432–443
60. Arispe, N., Pollard, H. B., and Rojas, E. (1994) *Mol. Cell. Biochem.* **140,** 119–125
61. Sanderson, K. L., Butler, L., and Ingram, V. M. (1997) *Brain Res.* **744,** 7–14

β-Amyloid Directly Inhibits Human α4β2-Nicotinic Acetylcholine Receptors Heterologously Expressed in Human SH-EP1 Cells

Jie Wu, Yen-Ping Kuo, Andrew A. George, Lin Xu, Jun Hu and Ronald J. Lukas

J. Biol. Chem. 2004, 279:37842-37851.
doi: 10.1074/jbc.M400335200 originally published online July 2, 2004
